JACS
JOURNAL OF THE AMERICAN CHEMICAL SOCIETY
Article
pubs.acs.org/JACS

Mutual Exclusivity in the Synthesis of High Crystallinity and High Yield Single-Walled Carbon Nanotubes

Hiroe Kimura,[†,‡,∥] Don N. Futaba,[†,‡] Motoo Yumura,[†,‡] and Kenji Hata*[,†,‡,§,∥]

[†]Technology Research Association for Single Wall Carbon Nanotubes (TASC), Tsukuba 305-8565, Japan
[‡]Nanotube Research Center, National Institute of Advanced Industrial Science and Technology (AIST), Tsukuba 305-8565, Japan
[§]Japan Science and Technology Agency (JST), Kawaguchi 332-0012, Japan
[∥]Department of Pure and Applied Sciences, Tsukuba University, Tsukuba 305-8573, Japan

Supporting Information

ABSTRACT: We report the mutually exclusive relationship between carbon nanotube (CNT) yield and crystallinity. Growth conditions were optimized for CNT growth yield and crystallinity through sequential tuning of three input variables: growth enhancer level, growth temperature, and carbon feedstock level. This optimization revealed that, regardless of the variety of carbon feedstock and growth enhancer, the optimum conditions for yield and crystallinity differed significantly with yield/crystallinity, preferring lower/higher growth temperatures and higher/lower carbon feedstock levels. This mutual exclusivity stemmed from the inherent limiting mechanisms for each property.

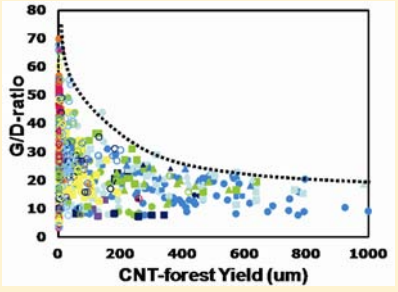

INTRODUCTION

Synthesis has always been one of the major limiting factors for every aspect of carbon nanotubes (CNTs) for both scientific research and industrial use. Therefore, numerous studies have been conducted to control the growth structure and improve the growth efficiency of CNT synthesis, e.g. to increase yield[1−8] and crystallinity[9−12] and to achieve chiral selectivity[13] and metal-semiconductor selective growth,[14,15] etc. Apt examples include the water-assisted chemical vapor deposition method to increase yield,[2] the floating catalyst chemical vapor deposition (CVD) method to improve crystallinity,[11] and catalyst gas pretreatments for metal conductor selective growth.[15]

It is interesting to note that most, if not all, previous CNT synthesis work has primarily focused on the control or improvement of a single aspect of the synthesis, such as growth yield or chirality control. However, to truly extract the full potential of CNTs and realize commercial applications, the achievement of only a single aspect is insufficient. For example, highly crystalline single-walled carbon nanotubes (SWCNT) made by arc discharge would be ideal for fibers, but due to their low productivity (yield), it is not likely that this fiber would be mass produced. Similarly, SWCNTs made in high yield would seem ideal for electrical, thermal, or mechanical connection, but the low crystallinity would degrade their properties. Among the various features of CNT synthesis, yield and crystallinity are the most essential aspects for CNTs to fulfill their industrial promise. High CNT yield is important from mere economic considerations, while high crystallinity is necessary to realize optimum performance. As such, a synthesis which could simultaneously realize CNTs with both high yield and high crystallinity would greatly drive the CNT field forward, thus being the ultimate goal for CNT synthesis. This conundrum is even more severe for SWCNTs because of the low growth efficiency compared to that of multiwalled carbon nanotubes (MWCNTs).

Despite the importance of yield and crystallinity, a literature survey revealed that these two important features have not yet been achieved simultaneously, and rather, the majority of the mainstream CNT synthesis reports show that a trade-off exists between the quality and the quantity. Simply put, when SWCNTs are synthesized in high quantity, the quality (crystallinity) dropped, and the achievement of both has not yet been reported. For example, laser ablation and arc discharge methods have both produced high crystallinity CNTs.[9−12] However, the production yield is limited to the kilogram scale. Another example is floating catalyst chemical vapor deposition (CVD), which can produce high crystallinity CNTs that can be processed into fibers stronger than those made by using carbon fibers.[16] However, the growth yield for such methods is very low, ∼6 g/h,[17] and this aspect hinders prospects for mass production. In contrast, attempts to increase the production yield of SWCNT, such as rotary kiln and fluidized bed CVDs, that have enabled economical production of MWCNTs with very high yield, on the hundreds of tons-per-year scale, have seen increases in the defect density.[6] Another example is water-assisted CVD, whereby with the addition of a growth enhancer the growth ambient has greatly improved the growth efficiency, enabling the synthesis of vertically aligned SWCNTs.[2] This method has been scaled-up to a pilot production plant where large growth substrates are continuously conveyed through the reactor, enabling annual ton-scale SWCNT production

Received: January 24, 2012
Published: May 16, 2012

dx.doi.org/10.1021/ja300769j | J. Am. Chem. Soc. 2012, 134, 9219−9224

previously unobtainable. However, the weakness of this approach is that the crystallinity is lower than that synthesized by other CVD techniques, such as floating catalyst CVD.[11]

In this article, we address this fundamental issue where the growth of vertically aligned SWCNT forests was optimized for both growth yield and crystallinity. Through applying an iterative optimization scheme to improve yield and crystallinity for water-assisted CVD, we found that not only were the respective optimized conditions different but also a mutual exclusive relationship between the yield and crystallinity was revealed. The yield/crystallinity preferred lower/higher growth temperatures and higher/lower carbon feedstock levels regardless of the carbon feedstock and growth enhancer.

RESULTS AND DISCUSSION

In this work we used the water-assisted CVD method as the basic synthetic technique, as it represents the CVD method with the highest growth efficiency (yield) per time and catalyst amount. Therefore, we pursued the possibility of improving the crystallinity while preserving the growth yield, from which we found the mutually exclusive relationship between yield and crystallinity. Our basic strategy was to incorporate the CNT synthesis into a feedback system whereby the outputs were optimized by sequentially optimizing the input levels. The three input parameters of water-assisted CVD were defined as the growth enhancer level, growth temperature, and carbon feedstock level. Similarly, the two CVD outputs were selected as the growth yield (represented by the height of the forests) and crystallinity (as measured by the G/D-ratio by Raman spectroscopy). Specifically, for a fixed growth temperature and ethylene level, the growth enhancer level was optimized. This typically required approximately four growths. After changing the growth temperature with the ethylene level remaining fixed, this process of optimizing the yield or G/D-ratio by adjusting the growth enhancer level was repeated. Nine temperatures were used spanning 700−900 °C. Finally, this process of ~36 growths was repeated for five different ethylene levels spanning 0.1−10%. After ~200 growths, the global and local maxima in the growth yield and crystallinity, as well as the relationship with the growth temperature and ethylene level, were found.

In the standard supergrowth process, SWCNT forests were synthesized in a 1 in. fully automated CVD furnace using a C_2H_4 carbon feedstock (~100 sccm), water (50−500 ppm) growth enhancer, and He with H_2 as a carrier gas (total flow 1 L per minute) with a growth time of 10 min. Fe (1 nm)/Al_2O_3 (40 nm) was sequentially sputtered on 2 × 2 cm silicon substrates.[2] Formation of nanoparticles for all cases was performed under the same conditions, He/H_2 and temperature 750 °C, to eliminate the catalyst formation step as a variable; then the temperature was adjusted to the growth temperature: ranging from 725 to 900 °C.

We found that, individually, both the growth yield and the crystallinity could be significantly improved by this growth optimization as shown in Figure 1. To address this point, a number of growths performed at a fixed ethylene concentration with various growth temperatures and growth enhancer levels were classified as a growth "family" as shown in the insets and open circles enclosed by the dashed loop in Figure 1b,c. Similarly, a number of growths at fixed growth temperature with various ethylene and growth enhancer levels were also performed. To represent the family, the highest yield/crystallinity output was selected and plotted as a large solid dot (Figure 1b−e). By connecting these peak outputs for each

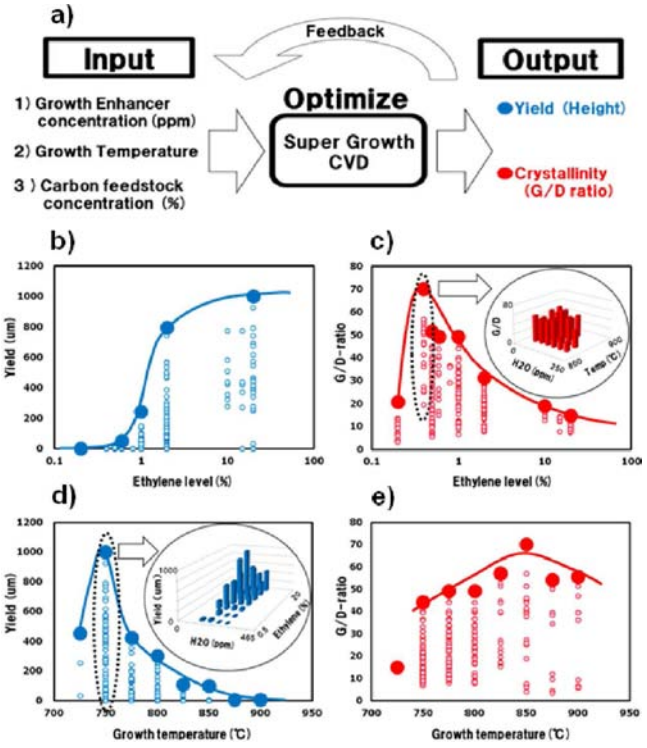

Figure 1. Optimization of yield and crystallinity. (a) Conceptual schematic of the input and output of the optimization scheme; (b) yield and (c) G/D-ratio as a function of ethylene level (%) (inset: 2-D plot of the G/D-ratio as a function of the humidity level and growth temperature); (d) yield and (e) G/D-ratio as a function of growth temperature (inset: 2-D plot of the yield as a function of the humidity and ethylene level).

family (blue, yield; red, crystallinity), the dependency of the output on the ethylene level/growth temperature became visually obvious.

By this analysis, we found that the optimum growth input conditions for SWCNT forest yield and crystallinity greatly differed. First, for ethylene level, the crystallinity showed a distinct peak at ~0.5% ethylene level where the G/D-ratio reached ~70 (Figure 1c). In stark contrast, the yield initially exhibited a proportional increase with the ethylene levels followed by a gradual saturation (Figure 1b). We note that the behavior of the yield was similar to the self-limited growth of biological systems, which is characterized by a region of unimpeded growth (upswing) followed by a bottlenecked growth (saturation). Therefore, higher ethylene level was preferred for growth yield while lower ethylene level was preferred for high crystallinity. Second, for growth temperature, both the SWCNT yield and crystallinity showed peaks but at significantly different temperatures (Figure 1d,e). The CNT forest yield showed a sharp increase from 725 to 750 °C, peaking distinctly at ~750 °C, where the yield doubled followed by a similarly sharp decrease (Figure 1d). In comparison, while still exhibiting a peak, the peak for crystallinity was much less sharp and occurred at a higher temperature (850 °C) (Figure 1e). These results showed that the optimum temperatures for yield and crystallinity were ~100 °C apart.

Summarizing, when optimized for yield, the ethylene level was ~10%, and the growth temperature was ~750 °C with a yield of ~1 mm and G/D-ratio of <10. On the other hand,

dx.doi.org/10.1021/ja300769j | J. Am. Chem. Soc. 2012, 134, 9219−9224

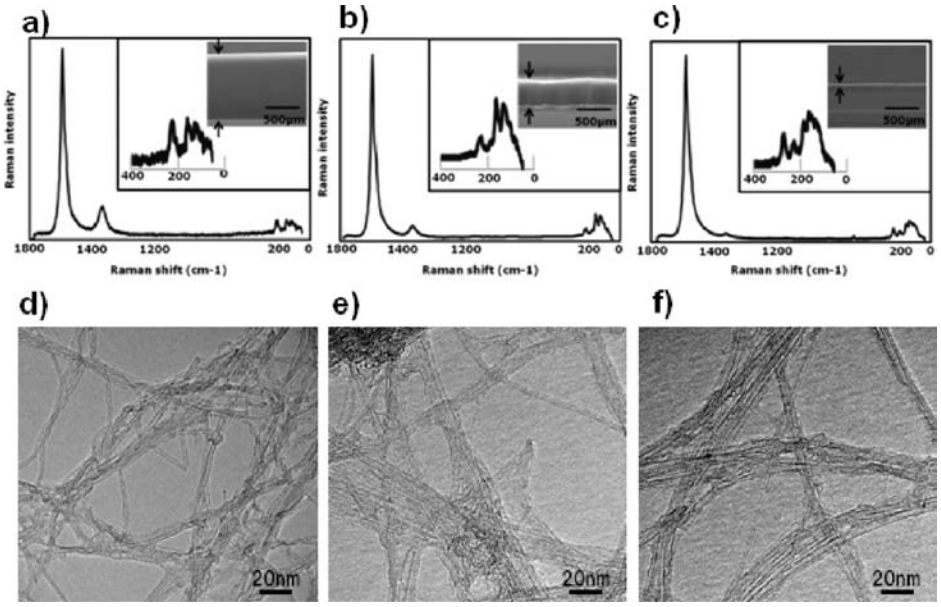

Figure 2. Characterization of the SWCNTs. (a) Raman spectra of the SWCNT forests at optimized yield conditions; (b) intermediate conditions; and (c) optimized crystallinity conditions. (Insets: radial breathing mode profiles, SEM image.) (d–f) Corresponding TEM images for parts a–c, respectively.

when optimized for crystallinity, the ethylene level was ~0.5%, and growth temperature was ~850 °C with a yield of ~10 μm and G/D-ratio of ~70. We would like to note that the aspect of improving crystallinity may not have been recognized in the past, as most research on CNT forests tends to focus on achieving higher yield.[1−7] These results clearly showed that higher temperature and lower ethylene levels were preferred for higher crystallinity, while lower temperatures and higher ethylene levels were preferred for higher yield. G/D-ratios exceeding 70 and beyond 200 have been reported by arc discharge, laser ablation, and floating catalyst CVD.[9−12] It is interesting to note that the growth temperature in these methods far exceeds 1000 °C, and our results imply that the general trend of increased temperature for increased crystallinity applied to other growth methods. Furthermore, this demonstrates the difficulty in concurrently achieving both high crystallinity and high growth yield by this growth technique.

We interpret that the difference in the optimum growth conditions for yield and crystallinity stems from the difference in the rate-limiting mechanisms, i.e. carbon conversion into CNTs and catalyst deactivation for yield and the incorporation of carbon into a low defect density lattice for crystallinity. For yield, above ~5% ethylene, a bottleneck effect was observed where other mechanisms (e.g., carbon conversion) and reaction pathways (e.g., catalyst deactivation through carbon coating) began to compete with the synthesis pathway. This showed that the catalysts had not yet exceeded their ability to convert ethylene to CNTs prior to deactivation. However, for crystallinity, the rate limiting step of carbon incorporation into a low defect density hexagonal lattice occurred at a significantly lower ethylene level (~0.5%), where the growth rates were still low. Similarly, with increased growth temperature, the observation of peaks indicates that both the yield and crystallinity suffered from their respective rate limiting steps.

The SWCNTs synthesized at optimized growth conditions for yield and crystallinity were characterized by Raman spectroscopy and transmission electron microscopy (TEM). Macroscopic Raman spectra (532 nm) for CNT forests optimized for yield and for crystallinity showed similarly sharp G-bands at ~1590 cm^{-1}, but the CNT forest optimized for crystallinity exhibited a significant drop in the D-band (Figure 2a–c). Hence, the G/D-ratio showed a 10-fold increase (~7 to ~70). In accordance, TEM examination of the three forests showed that the forests optimized for crystallinity exhibited greater straightness. In addition, TEM confirmed that all samples were SWCNTs, and radial breathing mode (RBM) peak profiles, which are related to the SWCNT diameter,[18] were similar. Therefore, it is less likely that differences in crystallinity and yield originated from changes in the CNT wall number or diameter. This is important because wall number and diameter are empirically known to affect yield and crystallinity. Furthermore, TEM observation showed that both samples showed minimal carbonaceous impurities, which is also known to affect the G/D-ratio. The CNT forest synthesized in this work falls within the high purity regime; therefore, we do not expect significant effects from non-CNT carbon content.

To confirm the generality of the observed difference in the optimized growth conditions for yield and crystallinity, we repeated the same experiments with two additional carbon feedstocks (acetylene, 1,3-butadiene) and another growth enhancer (CO_2). Recent developments of highly efficient CNT growth have shown that water-assisted CVD could be generalized to any carbon feedstock and growth enhancer given that the carbon source did not contain oxygen and the growth enhancer contained oxygen.[19] Therefore, we were interested to understand how the relative behavior of yield and crystallinity would change with a different growth ambient, because it had been reported that even slight changes in the growth ambient could result in changes in the structure.[20] We chose these particular carbon feedstocks because they were known not to change the CNT structure, such as wall number.[20] We repeated the optimization process for these additional sources and growth enhancer, and thus the result herein represents the culmination of more than 1000 CVD growths.

dx.doi.org/10.1021/ja300769j | J. Am. Chem. Soc. 2012, 134, 9219−9224

In general the optimized growth conditions and behavior with carbon feedstock level and growth temperature were similar regardless of the species of carbon feedstock and growth enhancer (Figure 3). First, for the carbon feedstock level, similar with ethylene, the yields using both acetylene and 1,3-butadiene showed proportional increases and eventual saturation with increased levels (Figure 3a). However, acetylene tended to saturate at lower input levels and at lower yields, while 1,3-butadiene demonstrated nearly the same upswing as ethylene but with a higher yield at saturation. Similarly, the G/D-ratio for each carbon source followed the same behavior as ethylene, yet acetylene and 1,3-butadiene again shifted toward lower carbon feedstock levels (Figure 3b). It should be noted that peaks were not observed for acetylene and 1,3-butadiene due to control limitations for gases, respectively. As in the case of ethylene, a higher feedstock level was preferred for growth yield while a lower feedstock level was preferred for high crystallinity. Second, for growth temperature, all carbon sources exhibited peaks with respect to the yield and G/D-ratio, yet again with small variances in peak location and height. The yields for both acetylene and 1,3-butadiene peaked at slightly higher temperatures than those for ethylene (775 °C vs 750 °C) (Figure 3c). Besides the difference in peak growth temperature, acetylene was nearly identical to ethylene with respect to peak shape and height while 1,3-butadiene differed additionally with a lower optimized yield. For crystallinity, despite differences in peak growth temperatures, the behaviors were all similar with the exception of an absence of a peak for acetylene within the tested region (Figure 3d). Therefore, despite the differences in carbon feedstocks, yield always showed a preference toward more moderate temperatures, and crystallinity showed a preference toward higher temperatures. Third, using CO_2 as the growth enhancer, in place of H_2O, with an ethylene carbon feedstock, no strong upswing in yield was observed in contrast when using H_2O (Figure 3e). However, the G/D peak profile, location, and height were nearly identical for both cases. For the growth temperature, the peak for CO_2 was broader, lower, and shifted upward ~25 °C (Figure 3f). The G/D-ratios for both cases were broad, but the peak for CO_2 was shifted to 100 °C lower temperatures. This showed that the optimum growth temperatures for both yield and crystallinity could match with the appropriate growth enhancer, but as a whole, these results showed that, regardless of the growth ambient, crystallinity and yield could not be simultaneously achieved.

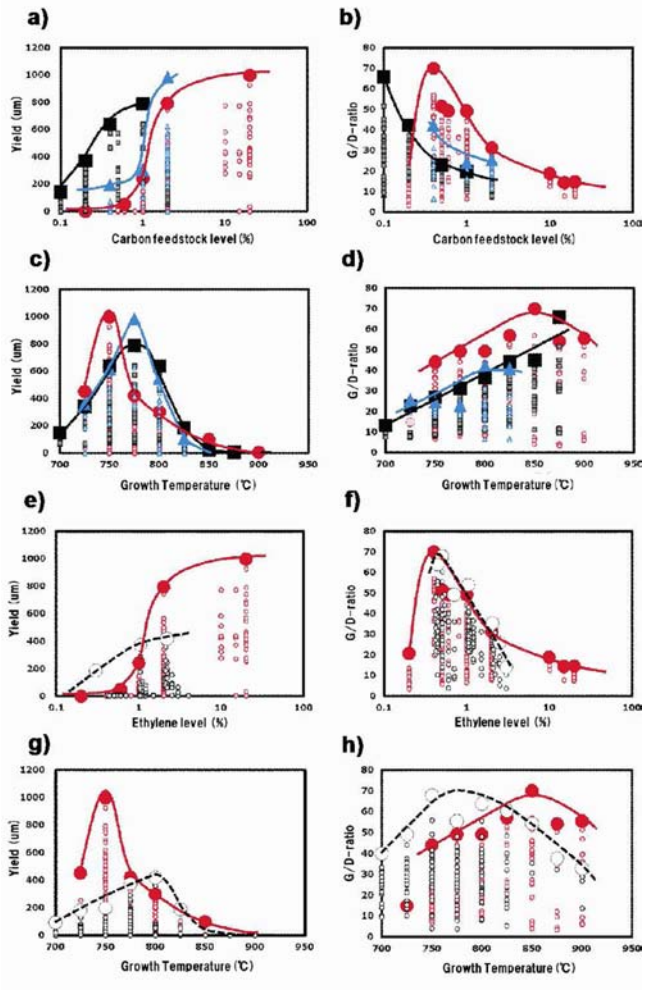

Figure 3. Generality toward different other carbon feedstocks and growth enhancers. (a) Yield and (b) G/D-ratio as a function of carbon feedstock level (%) for different carbon feedstocks. (c) Yield and (d) G/D-ratio as a function of growth temperature for different carbon feedstocks (red circles, ethylene; black squares, acetylene; blue triangles, 1,3-butadiene). (e) Yield and (f) G/D-ratio as a function of carbon feedstock level (%) for different growth enhancers. (g) Yield and (h) G/D-ratio as a function of growth temperature for different growth enhancers (red circles, ethylene + H_2O; open circles, ethylene + CO_2).

All of our CVD results were plotted into a two-dimensional map between growth yield versus crystallinity to show the relationship between two output properties, which we denote as a CVD "Ashby map" (Figure 4). (In material science, Ashby maps are simply plots of one material property versus another to show their mutual relationship.) We mapped hundreds of forests spanning diverse growth temperatures, growth enhancer (H_2O, CO_2) levels, and carbon feedstock (ethylene, acetylene, 1,3-butadiene) levels. Such a plot is commonly used to show the performance of a material or device, such as the well-known Ragone plot for energy devices where the energy density is plotted as a function of power density. The CVD Ashby map

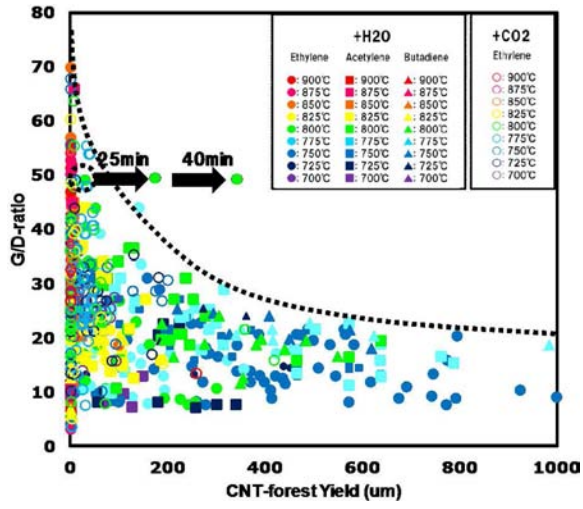

Figure 4. Mutual exclusivity of yield and crystallinity. CNT Ashby map of the crystallinity (G/D-ratio) and yield. Arrows indicate extension of the yield at increased crystallinity by extension of growth time.

dx.doi.org/10.1021/ja300769j | J. Am. Chem. Soc. 2012, 134, 9219–9224

clearly revealed the mutual exclusivity between high growth yield and crystallinity, and this observation constitutes our central finding. A trade-off exists between the yield and crystallinity, where generally the highest/lowest G/D-ratios correspond to the shortest/tallest forests. In addition, as the yield increased, the G/D-ratio appeared to asymptotically approach ~7. This data shows that the growth condition could be tuned for an individual output; however, simultaneously tuning multiple outputs appeared inherently impossible within this specific CVD technique. We interpret that this inverse relationship stems from two basic mechanisms: first, the inability of the carbon atoms to be incorporated into a perfect graphene lattice at high CNT growth rates; second, the inability to relieve stress at the CNT−catalyst interface during the growth process due to contact with neighboring CNTs. This may also explain why MWCNTs tend to possess poorer crystallinity than that of SWCNTs. It is interesting to note that all the results discussed herein were taken from a fixed growth time of 10 min. The drop in the growth yield is a direct result of the low carbon feedstock levels and therefore low growth rate. While generally the extension of the growth time is not necessarily a prudent approach to increase forest height as the carbon impurities increase with increased exposure to the growth ambient,[21] we found that the growth time could be extended to 25 and 40 min, while maintaining a G/D-ratio of 50, and the yield increased to ~200 and ~370 μm, respectively (Figure 4).

This mutual exclusivity explains why our literature survey of yield and crystallinity research fell into two groups (high crystallinity/low yield and low crystallinity/high yield), and that, despite advances in synthesis, it remains a limiting factor for controlling two key structures: crystallinity and high yield. Our results provide a fundamental understanding of the relationship between crystallinity and yield and therefore offer promising directions to achieve high yield and high crystallinity. One approach would be to tailor the catalyst and carbon feedstock so that the optimum growth temperatures and carbon feedstock levels could be made to coincide. This could be done by controlling the carbon solubility and melting points of the catalysts and the decomposition rate of the carbon feedstock. A completely different route would be not to attempt to achieve both high yield and crystallinity by CVD synthetic means, but to separate the processes, such as for carbon nanofibers. A number of processes have been reported to improve the crystallinity following the synthesis.[22−24] Here, the challenge would be to categorize the defects in terms of their ease of removal by the post process and to control the growth to not include defects which are difficult to eliminate.

SUMMARY

In summary, we have demonstrated the mutually exclusive relationship between yield and crystallinity though applying an iterative optimization scheme to improve yield and crystallinity for water-assisted CVD. The fundamental mechanisms required for both output properties resulted in different optimized conditions for crystallinity and yield. While these results were specific for the water-assisted and the growth-enhancer assisted CVD techniques, we believe that these results are general, as the mechanisms limiting crystallinity and yield are general to all CNT synthesis techniques, i.e. carbon conversion to CNTs and catalyst activity required for high yield and carbon incorporation into a highly defect-free lattice for high crystallinity.

METHODS

Raman spectroscopic characterization was performed using a Thermo-Electron Raman Spectrometer with an excitation wavelength of 532 nm and a macroscopic sampling diameter of 0.3 mm.

ASSOCIATED CONTENT

Supporting Information

CNT yield as a function of ethylene level (%); G/D-ratio as a function of ethylene level (%); 2-D plot of the G/D-ratio as a function of the humidity level and growth temperature; yield as a function of growth temperature; 2-D plot of the yield as a function of the humidity level and ethylene level (%); G/D-ratio as a function of growth temperature; and spatially resolved Raman spectra as a function of depth from the forest top. This material is available free of charge via the Internet at http://pubs.acs.org.

AUTHOR INFORMATION

Corresponding Author

kenji-hata@aist.go.jp

Notes

The authors declare no competing financial interest.

ACKNOWLEDGMENTS

We acknowledge support from the Nanotechnology Program "Carbon Nanotube Capacitor Development Project" (2006−2011) by the New Energy and Industrial Technology Development Organization ("NEDO").

REFERENCES

(1) Nikolaev, P.; Bronikowski, M. J.; Bradley, R. K.; Rohmund, F.; Colbert, D. T.; Smith, K. A.; Smalley, R. E. *Chem. Phys. Lett.* **1998**, *313*, 91.

(2) Hata, K.; Futaba, D. N.; Mizuno, K.; Namai, T.; Yumura, M.; Iijima, S. *Science* **2004**, *306*, 1362−1365.

(3) Zhong, G.; Iwasaki, T.; Robertson, J.; Kawarada, H. *J. Phys. Chem. B* **2007**, *111*, 1907−1910.

(4) Hart, A. J.; Slocum, A. H. *J. Phys. Chem. B* **2006**, *110*, 8250−8257.

(5) Kayastha, V. K.; Wu, S.; Moscatello, J.; Yap, Y. K. *J. Phys. Chem. C* **2007**, *111*, 10158−10161.

(6) Hernadi, K.; Fonseca, A.; Nagy, J. B.; Bernaerts, D.; Lucas, A. *Carbon* **1996**, *34*, 1249−1257.

(7) Hasegawa, K.; Noda, S. *Jpn. J. Appl. Phys.* **2010**, *49*, 085104-1−085104-6.

(8) Chakrabarti, S.; Gong, K.; Dai, L. *J. Phys. Chem. C* **2008**, *112*, 8136.

(9) Ebbesen, T. W.; Ajayan, P. M. *Nature* **1992**, *358*, 220−222.

(10) Thess, A.; Lee, R.; Nikolaev, P.; Dai, H.; Petit, P.; Robert, J.; Xu, C.; Lee, Y. H.; Kim, S. G.; Rinzler, A. G.; Colbert, D. T.; Scuseria, G. E.; Tomfinek, D.; Fischer, J. E.; Smalley, R. C. *Science* **1996**, *273*, 48.

(11) Saito, T.; Ohshima, S.; Okazaki, T.; Ohmori, S.; Yumura, M.; Iijima., S. *J. Nanosci. Nanotechnol.* **2008**, *8*, 6153−6157.

(12) Moisala, A.; Nasibulin, A. G.; Brown, D. P.; Jiang, H.; Khriachtchev, L.; Kauppinen, E. I. *Chem. Eng. Sci.* **2006**, *61*, 4393−4402.

(13) Bachilo, S. M.; Balzano, L.; Herrera, J. E.; Pompeo, F.; Resasco, D. E.; Weissman, R. B. *J. Am. Chem. Soc.* **2003**, *125*, 11186−11187.

(14) Li, Y. M.; Mann, D.; Rolandi, M.; Kim, W.; Ural, A.; Hung, S.; Javey, A.; Cao, J.; Wang, D. W.; Yenilmez, E.; Wang, Q.; Gibbons, J. F.; Nishi, Y.; Dai, H. J. *Nano Lett.* **2004**, *4*, 317−321.

(15) Harutyunyan, A. R.; Chen, G.; Paronyan, T. M.; Pigos, E. M.; Kuznetsov, O. A.; Hewaparakrama, K.; Kim, S. M.; Zakharov, D.; Stach, E. A.; Sumanasekera, G. U. *Science* **2009**, *326*, 116−120.

(16) Motta, M.; Moisala, A.; Kinloch, I.; Windle, A. H. *Adv. Mater.* **2007**, *19*, 3721−3726.
(17) Ying, L. S.; Salleh, M. A. b. M.; Yusoff, H. b. M.; Rashid, S. b. A.; Razak, J. b. A. *J. Ind. Eng. Chem.* **2011**, *17*, 367−376.
(18) Milnera, M.; Kurti, J.; Hulman, M.; Kuzmany, H. *Phys. Rev. Lett.* **2000**, *84*, 1324.
(19) Futaba, D. N.; Goto, J.; Yasuda, S.; Yamada, T.; Yumura, M.; Hata, K. *Adv. Mater.* **2009**, *21*, 4811−4815.
(20) Futaba, D. N.; Goto, J.; Yasuda, S.; Yamada, T.; Yumura, M.; Hata, K. *JACS* **2009**, *131*, 15992−15993.
(21) Yasuda, S.; HIraoka, T.; Futaba, D. N.; Yamada, T.; Hata, K. *Nano Lett.* **2009**, *9*, 769−773.
(22) Chiang, I. W.; Brinson, B. E.; Smalley, R. E.; Margrave, J. L.; Hauge, R. H. *J. Phys. Chem. B* **2001**, *105*, 1157−1161.
(23) Yudasaka, M.; Ichihashi, T.; Kasuya, D.; Kataura, H.; Iijima, S. *Carbon* **2003**, *41*, 1273−1280.
(24) Jensen, K.; Mickelson, W.; Han, W.; Zettl, A. *Appl. Phys. Lett.* **2005**, *86*, 173107−173109.